JVI Journals.ASM.org

Interaction between Shadoo and PrP Affects the PrP-Folding Pathway

Danica Ciric,[a] Charles-Adrien Richard,[a] Mohammed Moudjou,[a] Jérôme Chapuis,[a] Pierre Sibille,[a] Nathalie Daude,[b] David Westaway,[b] Miguel Adrover,[c] Vincent Béringue,[a] Davy Martin,[a] Human Rezaei[a]

National Institute for Agricultural Research (INRA), Pathological Macro-Assemblies and Prion Pathology Group (MAP[2]), UR892, Virologie Immunologie Moléculaires, Jouy-en-Josas, France[a]; University of Alberta, Centre for Prion and Protein Folding Diseases, Research in Neurodegenerative Diseases, Edmonton, AB, Canada[b]; Institut Universitari d'Investigació en Ciències de la Salut (IUNICS), Departament de Química, Universitat de les Illes Balears, Palma de Mallorca, Spain[c]

ABSTRACT

Prion diseases are characterized by conformational changes of a cellular prion protein (PrP^C) into a β-sheet-enriched and aggregated conformer (PrP^{Sc}). Shadoo (Sho), a member of the prion protein family, is expressed in the central nervous system (CNS) and is highly conserved among vertebrates. On the basis of histoanatomical colocalization and sequence similarities, it is suspected that Sho and PrP may be functionally related. The downregulation of Sho expression during prion pathology and the direct interaction between Sho and PrP, as revealed by two-hybrid analysis, suggest a relationship between Sho and prion replication. Using biochemical and biophysical approaches, we demonstrate that Sho forms a 1:1 complex with full-length PrP with a dissociation constant in the micromolar range, and this interaction consequently modifies the PrP-folding pathway. Using a truncated PrP that mimics the C-terminal C1 fragment, an allosteric binding behavior with a Hill number of 4 was observed, suggesting that at least a tetramerization state occurs. A cell-based prion titration assay performed with different concentrations of Sho revealed an increase in the PrP^{Sc} conversion rate in the presence of Sho. Collectively, our observations suggest that Sho can affect the prion replication process by (i) acting as a holdase and (ii) interfering with the dominant-negative inhibitor effect of the C1 fragment.

IMPORTANCE

Since the inception of the prion theory, the search for a cofactor involved in the conversion process has been an active field of research. Although the PrP interactome presents a broad landscape, candidates corresponding to specific criteria for cofactors are currently missing. Here, we describe for the first time that Sho can affect PrP structural dynamics and therefore increase the prion conversion rate. A biochemical characterization of Sho-PrP indicates that Sho acts as an ATP-independent holdase.

Prion diseases, such as bovine spongiform encephalopathy and Creutzfeldt-Jakob disease, are characterized by conformational changes of a cellular prion protein (PrP^C) into a β-sheet-enriched abnormal isoform (PrP^{Sc}). The biosynthesis of PrP^C is necessary for the pathogenesis of prion diseases, and PrP-knockout mice are resistant to these diseases (1). The conversion of PrP^C into PrP^{Sc} is a crucial event in prion replication, and PrP^{Sc} is further able to act as a template for the conformational change of PrP^C.

The Shadoo (Sho) protein is a member of the PrP protein family; however, the sequence homology between Sho and PrP is restricted to the internal hydrophobic domain (PrP residues 106 to 126). Physiologically, Sho exhibits neuroprotective properties similar to those of PrP^C (2), and these proteins share a number of common binding partners (3). Transcriptome sequencing analyses performed on young embryos in which PrP and/or Sho had been inactivated indicate that these two proteins are involved in embryonic development (4). Although these observations suggest that Sho and PrP may be functionally related (5, 6), it remains unclear whether the absence of PrP could be compensated for by Sho at early developmental stages (7, 8).

Similar to PrP, recombinant mouse and sheep Sho proteins are able to form amyloid assemblies (9). In addition, decreased levels of endogenous Sho may be an indicator of an early response to PrP^{Sc} accumulation in the central nervous system (CNS) hundreds of days prior to the onset of neurological symptoms (10). A direct interaction between Sho and PrP involving the segment from residues 61 to 77 of Sho and the segment from residues 108 to 126 of PrP, determined by the yeast two-hybrid assay, has been reported (11). However, the contribution of this interaction to the evolution of prion pathology or to the folding pathway of PrP remains uncertain.

To determine whether Sho can directly affect the PrP-folding pathway and, consequently, its conversion process, we first characterized the interaction between Sho and different truncated forms of PrP. We observed that full-length PrP and its N-terminal segment form a 1:1 complex with Sho, whereas the C-terminal segment displays a cooperative binding behavior. By exploring the PrP oligomerization process in the presence of Sho, we show that this interaction drastically affects the PrP oligomerization pathway. Moreover, scrapie cell assays revealed an increase in the PrP^{Sc} conversion rate in the presence of Sho. Collectively, our results

Received 18 December 2014 **Accepted** 27 March 2015

Accepted manuscript posted online 8 April 2015

Citation Ciric D, Richard C-A, Moudjou M, Chapuis J, Sibille P, Daude N, Westaway D, Estelrich MA, Béringue V, Martin D, Rezaei H. 2015. Interaction between Shadoo and PrP affects the PrP-folding pathway. J Virol 89:6287–6293. doi:10.1128/JVI.03429-14.

Editor: B. W. Caughey

Address correspondence to Davy Martin, davy.martin@jouy.inra.fr, or Human Rezaei, human.rezaei@jouy.inra.fr.

doi:10.1128/JVI.03429-14

strongly suggest that Sho might affect the evolution of prion replication dynamics through its interaction with PrP.

MATERIALS AND METHODS

Reagents and antibodies. Reagents for SDS-PAGE and Western blot analyses were purchased from Bio-Rad (Nanterre, France). We used a rabbit anti-Sho polyclonal antibody (SPRN [R-12] antibody; Santa Cruz, Heidelberg, Germany) and horseradish peroxidase-conjugated anti-rabbit IgG (P.A.R.I.S. Compiègne, France) as a secondary antibody. Unless otherwise indicated, all other reagents were purchased from Sigma-Aldrich (Saint Quentin Fallavier, France).

Ethics statement. Animal experiments were carried out in strict accordance with EU directive 2010/63 and were approved by the INRA COMETHEA (permit number 12/034).

Protein construction and expression. The full-length mature ovine prion protein (reference sequence, GenBank accession number NP_001009481.1), named ARQ (amino acids 23 to 231), and different His-tagged truncated forms of the protein (proteins with deletions of residues 23 to 126 [PrP Δ23–126] and residues 106 to 231 [PrP Δ106–231]) were produced in *Escherichia coli* and purified as described previously (12). Purified monomeric PrPs were stored, lyophilized, and recovered in the desired buffer by elution through a G25 desalting column (GE Healthcare, Orsay, France).

Sho protein production. The gene encoding mature mouse Sho (amino acids 25 to 122; reference sequence, GenBank accession number NP_898970.1) was amplified by PCR, cloned into the pET-28 plasmid (Novagen, EMD Millipore, USA), and expressed in *Escherichia coli* SolBL21 (Genlantis, USA). Expression was induced for 6 h by adding 1 mM IPTG (isopropyl-β-D-thiogalactopyranoside) to Luria-Bertani medium supplemented with 40 mg/liter kanamycin at 37°C and agitating the mixture by spinning at 150 rpm. The bacteria were harvested, lysed in 10 mM Tris-HCl with 10 mM EDTA (pH 7.5) and 1% Triton X-100 for 30 min at 37°C, and then sonicated for 5 min on ice. After centrifugation (15 min at 15,000 × *g*), the obtained inclusion bodies were solubilized in 8 M urea buffer with 5 mM imidazole, 20 mM Tris, and 500 mM NaCl (pH 7.4) for 48 h at 4°C. After centrifugation (1 h at 15,000 × *g*), the supernatant was loaded onto a 5-ml HiTrap immobilized-metal affinity chromatography column charged with 0.2 M nickel sulfate and equilibrated with low-imidazole buffer (5 mM imidazole, 20 mM Tris-HCl [pH 7.4], 0.5 M NaCl, 8 M urea) using a 50-ml Superloop. Imidazole (40 mM) in the same buffer was applied to elute low-affinity, nonspecific, column-bound impurities. Finally, a linear gradient of 40 to 800 mM imidazole in the same buffer was applied to elute Sho fractions containing the His-tagged proteins. After equilibration with 20 mM Tris-HCl (pH 7.4), 0.5 M NaCl, and 8 M urea buffer, Shadoo was further purified by size exclusion chromatography on a HiLoad Superdex 200 column with a 120-ml total bed volume (GE Healthcare). The Superdex 200 column was calibrated with the following standard globular proteins from a gel filtration calibration kit (GE Healthcare): ferritin (440 kDa), catalase (232 kDa), bovine serum albumin (BSA; 67 kDa), ovalbumin (43 kDa), chymotrypsinogen A (25 kDa), and RNase A (13.7 kDa). In the third and final step, salts and urea were removed using a 53-ml HiPrep 26/10 desalting column (GE Healthcare), and the proteins were recovered in 5 mM ammonium acetate (pH 5) for lyophilization and storage. The identification of Sho was performed by matrix-assisted laser desorption ionization mass spectrometry. Proteins were labeled with Alexa Fluor 488 carboxylic acid, succinimidyl ester (Molecular Probes Inc., Life Technologies, USA), according to the manufacturer's recommendations, and the excess dye was removed by chromatography on a desalting column (HiTrap desalting column; GE Healthcare).

Microscale thermophoresis. Microscale thermophoresis is a technology that uses the motion of fluorescent molecules along a microscale temperature gradient to detect any changes in their hydration shell, which can be induced by the binding to a partner (13–16). A fixed concentration of labeled proteins (either 170 nM ARQ, 121 nM C terminus of ARQ, or 112.5 nM N terminus of ARQ) was incubated with increasing amounts of Shadoo in 20 mM MES (morpholineethanesulfonic acid; pH 6.5), 20 mM NaCl, and 2% BSA at room temperature for 15 min. The measurements were performed for 30 s using a Monolith NT.115 instrument (NanoTemper Technologies GmbH, Munich, Germany) at 20°C (blue LED laser power at 100% and infrared laser power at 40%). The data from three independent measurements were averaged and analyzed using the temperature-jump phase of NTAnalysis software (NanoTemper Technologies).

Cross-linking. Chemical cross-linking was performed using the homobifunctional *N*-hydroxysuccinimide ester EGS [ethylene glycol bis(succinimidyl succinate); Thermo Fisher Scientific Inc., USA]. The reaction was performed in 20 mM MES with 20 mM NaCl (pH 6.5) for 3 h. Proteins at a molar ratio of 1:1 (10 μM) were incubated for 30 min at 25°C before the addition of 0.5 mM, 1 mM, or 2 mM EGS, and the reaction was quenched with 50 mM Tris (pH 7.5) for 15 min. Cross-linked complexes were denatured, submitted to SDS-PAGE, and then stained with Coomassie brilliant blue G-250 for visualization (Bio-Rad Laboratories S.A., France).

DSC. Differential scanning calorimetry (DSC) thermograms were obtained using a MicroCal DSC instrument with cell volumes of 0.5 ml at scan rates of 60 and 90°C/h. All experiments were performed using full-length PrP and PrP Δ106–231 at 50 μM in 20 mM MOPS (morpholinepropanesulfonic acid buffer; pH 7.2). The DSC thermograms were analyzed with Origin Lab software.

Oligomerization test by exclusion chromatography. Conversion of PrP and Sho to oligomeric forms was performed in 20 mM MOPS (pH 7.0). PrP at a final concentration of 50 μM, a mixture of 50 μM PrP with 10 μM Sho, and 10 μM Sho alone were incubated in a PerkinElmer GenAmp2400 thermocycler at 65°C for 45 min. Homogeneous fractions of oligomers were then collected after separation by size-exclusion chromatography (SEC), and SEC was performed at 20°C using a TSK 4000SW (7 mm by 600 mm) gel filtration column (Interchim, Montluçon, France) with 20 mM sodium citrate (pH 3.35). Protein elution was monitored by measurement of UV absorption at 280 nm.

SLS. Static light-scattering (SLS) kinetics and temperature ramping experiments were performed with an in-lab device using 407-nm laser beams in a 2-mm-path-length quartz cuvette. Kinetic experiments were performed according to a standardized methodology, as previously reported (17): at 50°C in 20 mM MOPS (pH 7.0) with PrP and Sho concentrations of 50 μM and 10 μM, respectively. Due to the high sensitivity of the light-scattering technique, we fixed the concentration of Sho at 10 μM in order to prevent any nonspecific Sho aggregation. Temperature-ramping experiments were performed at a rate of increase in the temperature of 1°C/min, beginning from 15°C and going to 90°C, in 20 mM MOPS (pH 7.0).

CPT assay. The effect of Shadoo on PrP^{Sc} biosynthesis was estimated using a cell-based prion titration (CPT) assay. RK-13 cells were stably transfected with a P2F plasmid expressing ovine PrP variant V136 R154 Q171; the cells were later cloned to establish a stable cell line (to be published elsewhere) (18). The cells were grown at 37°C in a 5% CO_2–air atmosphere using Opti-MEM medium (Life Technologies, Inc.) supplemented with 10% fetal calf serum (FCS), 100 IU/ml of penicillin, and 100 mg/ml of streptomycin in 96-well plates. After the establishment of cell monolayers, the medium was replaced with fresh medium without FCS, and the cells were preincubated for 10 min with increasing concentrations of Sho (from 1.2 nM to 30 μM) before a 24-h incubation with either a 10^{-4} dilution ($10^{3.7}$ the 50% lethal dose [LD_{50}]) or a 10^{-3} dilution ($10^{2.7}$ LD_{50}) of 20% brain homogenate from terminally ill tg338 mice infected with the 127S strain (18). The strain 127S infectious titer is $10^{9.2}$ LD_{50}/g of tg338 mouse brain (19). After incubation, the medium was replaced with fresh Opti-MEM medium supplemented with 10% FCS, and the cells were grown for 10 days and then fixed for 10 min in 4% (wt/vol) paraformaldehyde (PFA)–4% sucrose in phosphate-buffered saline (PBS). The fixed cells were treated with 0.1% Triton X-100 and then with 3.5 M guanidine

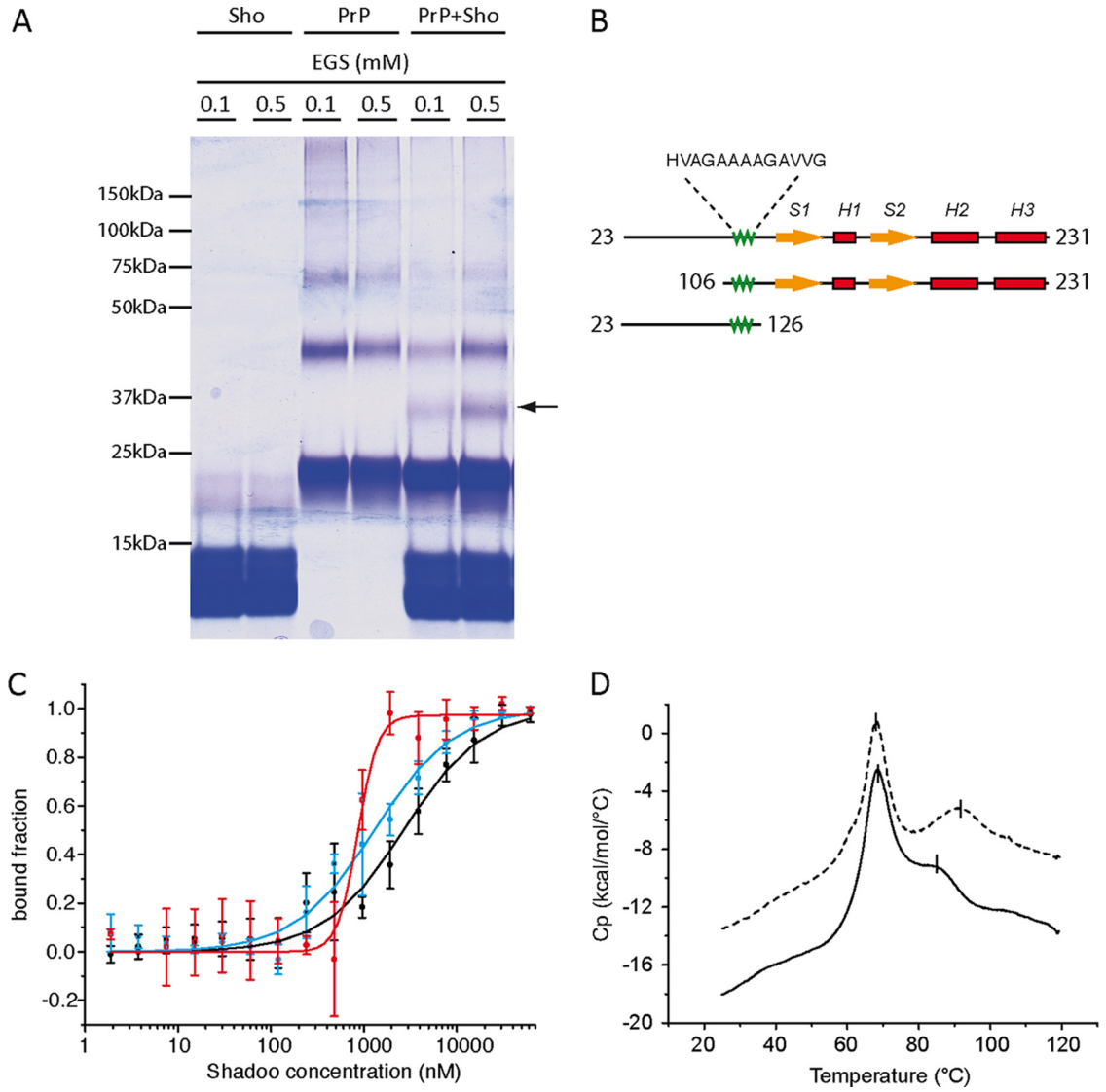

FIG 1 Characterization of the PrP-Sho interaction. (A) Results of EGS cross-linking experiments analyzed by SDS-PAGE. Treatment of monomeric PrP and Sho with EGS at 0.1 and 0.5 mM did not result in the appearance of additional bands. Incubation of PrP (10 μM) with 10 μM Sho in the presence of EGS resulted in an additional band (indicated by the arrow) with an apparent molecular mass corresponding to that of a 1:1 PrP-Sho heterodimer. (B) The different PrP constructions used for the MST experiments. (Top to bottom) Full-length PrP and the C-terminal and N-terminal domains of PrP, respectively. The green segment represents the previously reported putative Sho binding domain (11), which corresponds to the PrP segment from residues 106 to 126. H, helix domains; S, beta strands. (C) Results of MST experiments using Sho to titrate fluorescently labeled full-length PrP (black), the N-terminal domain from residues 23 to 126 (blue), and the C-terminal domain from residues 106 to 231 (red). The results are expressed as the means ± SDs from three different experiments. (D) Results of DSC experiments with full-length PrP (solid line) and the C-terminal domain from residues 106 to 231 (dash line). Cp, calorific capacity at constant pressure.

isocyanate. Immunofluorescent labeling was performed using the primary antibody ICSM33 (1:2,000) (20), which specifically detects PrP^{Sc}, followed by labeling with Alexa Fluor 488-conjugated secondary anti-mouse antibody (Abcam, France) at an initial concentration of 1:500 and DAPI (4′,6-diamidino-2-phenylindole) staining. The immunofluorescent PrP^{Sc} signal was acquired with an inverted fluorescence microscope (Zeiss Axiovision), and the signal was quantified per cell per well. Serial 10-fold dilutions of infected brain homogenates were prepared under the same conditions and run in parallel experiments to establish a tissue culture infectious dose curve that directly related to the PrP^{Sc} content; the standard deviation (SD) was established from triplicate measurements.

RESULTS

PrP and Sho interact in a 1:1 stoichiometry. PrP and Sho have been reported to interact in a double-hybrid system (11). To better characterize this interaction, we first performed cross-linking experiments using purified recombinant proteins (Fig. 1A, first and second lanes) and different concentrations of the cross-linking reagent EGS, followed by SDS-PAGE analysis. Analysis of Sho and PrP alone did not reveal any additional bands, even at a high EGS concentration (Fig. 1A, first to fourth lanes; PrP monomer, 22 kDa; Sho monomer, 13 kDa). However, when PrP and Sho were mixed at a 1:1 ratio in the presence of EGS, we observed the appearance of an additional band (35 kDa; Fig. 1A, fifth and sixth lanes), which corresponded to the formation of a 1:1 PrP-Sho heterodimer. We next studied the strength of this interaction by carrying out microscale thermophoresis (MST) measurements using either full-length or truncated, labeled forms of PrP in the

TABLE 1 PrP and Sho interaction

Segment	K_d/BC_{50} (μM)	Hill no.
PrP residues 23–231	2.6 ± 0.3	1 ± 0.1
N terminus (residues 23–126)	1.2 ± 0.1	1 ± 0.2
C terminus (residues 106–231)	0.9 ± 0.2	4 ± 0.6

presence of increasing amounts of Sho (Fig. 1B and C). The fitting of the data strongly suggested a 1:1 stoichiometry when full-length PrP and the N-terminal segment (residues 23 to 126) were used, and the dissociation constant (K_d) values were estimated to be 2.6 ± 0.3 μM and 1.2 ± 0.1 μM, respectively (Fig. 1C, black and blue lines, respectively, and Table 1). The difference between these two values suggests that the PrP C terminus has a reduced affinity for Sho, most likely due to steric hindrance. The titration curve constructed for the binding of Sho to the PrP C-terminal domain (residues 106 to 231) revealed a sharp sigmoid curve that suggested the cooperative binding of Sho (Fig. 1C, red line). Owing to this cooperativity, we could estimate the 50% binding concentration (BC_{50}) to be only 0.9 ± 0.1 μM with a Hill number of 4 (Table 1). These experiments show that PrP and Sho directly interact and that PrP contains a Sho binding site between residues 106 and 126. Altogether, these observations suggest that the PrP-Sho interaction demonstrates dual behavior. Sho forms a 1:1 complex both with full-length PrP and with the N-terminal segment of PrP; however, the absence of the N-terminal segment induces cooperative binding behavior, which suggests a structural rearrangement of the C-terminal segment and the formation of a quaternary structure during PrP C terminus-Sho binding. Rearrangement of the PrP C terminus is inhibited by the PrP N terminus and is essential for achieving the high-affinity binding of Sho to PrP.

To determine whether the dual behavior of Sho binding is a consequence of the modification of the PrP-folding pathway due to the presence or absence of the N-terminal segment, we explored the folding pathway of full-length PrP and of the PrP C-terminal domain using differential scanning calorimetry. As reported previously and shown in Fig. 1D, the full-length unfolding process followed a first transition, which corresponded to the unfolding of the native state, followed by a second transition, which corresponded to the melting of the oligomers produced during the unfolding process (17, 21). The observation that the melting temperature (T_m) of the second transition was significantly shifted upward in the case of the C-terminal domain suggested that the N-terminal domain affected the stability of the native state and/or the oligomerization pathway. Therefore, the nature of Sho binding is determined by the structural dynamics of PrP.

Sho affects the PrP oligomerization pathway. We previously reported that PrP oligomerization generates two populations of discrete oligomers (termed O1 and O3) via parallel pathways (17, 22). To determine whether the PrP-folding pathways are affected by the interaction of PrP with Sho, we explored the oligomerization process of PrP in the presence of Sho (Fig. 2). Under our experimental conditions at pH 7.0, O3 species were mainly formed in the absence of Sho (Fig. 2A, black line; elution volume, 15 ml). In the presence of Sho, the elution profile was broader and higher-molecular-mass species were formed (Fig. 2A, red line). This profile modification could have been due either to the presence of various concentrations of Sho in the O1 and O3 species or to the decreased formation of O3 in favor of O1. The presence of Sho in the fractions was monitored by SDS-PAGE, and Fig. 2B shows that Sho was associated with each oligomer. Therefore, Sho continued to bind to the PrP protomers to form heteroassemblies with PrP.

To more specifically determine the contribution of Sho to the PrP-folding pathway, the variation in the static light-scattering (SLS) signal intensity was monitored as a function of temperature. The SLS signal was used in these experiments to quantitatively detect all phase transitions involving variations in the quaternary structure. As shown in Fig. 2C (blue line), Sho alone did not form any quaternary structure that was detectable by SLS. In the case of PrP, the scattergram revealed two quaternary structure transitions, T_{m1} and T_{m2}, at 55°C and 71°C, respectively (Fig. 2C, black line), which corresponded to the melting temperatures of the O3 and O1 oligomers, respectively (23). The scattergram of the PrP-Sho (5:1 ratio) mixture (Fig. 2C, red line) displayed a similar intensity at transition T_{m1}, but without a temperature shift. Because the molecular mass of the O3 oligomers incorporating Sho partners should be higher, this experiment suggests that the amount of O3 was decreased in the presence of Sho. Hence, Sho slightly inhibits the formation of O3. However, because the temperature transition did not change, Sho does not affect the stability of this species. In contrast, the scattered light intensity was drastically decreased at transition T_{m2}, and for the same reason stated above, we concluded that Sho drastically inhibits the formation of O1. Moreover, as the transition temperature was shifted toward a higher temperature (T_{m2} = 76°C, compared with a T_{m2} of 71°C for O3), Sho stabilized the O1 complex or induced the formation of a new type of complex that was more stable than O1.

A decrease in the amount of complex formed could also result from slower complex formation kinetics. To investigate this possibility, we compared the oligomerization kinetics of PrP in the presence of Sho at 50°C (near the T_{m1} transition) to monitor the formation of both O1 and O3 (Fig. 2D). At this temperature, no variation in the scattered intensity was observed for Sho at 10 μM. However, a lower plateau was observed when Sho was present in the reaction mixture at a PrP/Sho ratio of 5:1, and two plateaus were reached at the same time in the presence or absence of Sho (10 min). Moreover, throughout the formation of the complexes, we observed a linear correlation between the scattered intensities (Fig. 2E) in the presence or absence of Sho. Thus, Sho does not affect the kinetic parameters but does affect the amount of complexes that are formed. Altogether, these experiments show that Sho does not affect the O3 oligomerization pathway much, but it drastically affects the O1 oligomerization pathway by inducing the formation of a complex with a more stable quaternary structure.

Sho affects the formation of PrP^{Sc}. Previous experiments suggested that PrP and Sho are able to form a heterocomplex that affects the PrP-folding landscape. To determine whether Sho is able to interfere with the prion replication process, we performed a cell-based prion titration (CPT) assay in the presence of Sho. Cells were preincubated with various concentrations of purified recombinant Sho and then infected with a 10^{-3} or a 10^{-4} dilution of a strain 127S-infected brain homogenate; the cells were then incubated for 11 days, and their PrP^{Sc} content was analyzed (n = 3 experiments performed in triplicate). PrP^{Sc} quantification by immunofluorescence revealed a pseudo-Gaussian shape of the PrP^{Sc} quantity as a function of the concentration of Sho. At the 10^{-3} dilution, there was a 2-fold increase in the levels of PrP^{Sc} for

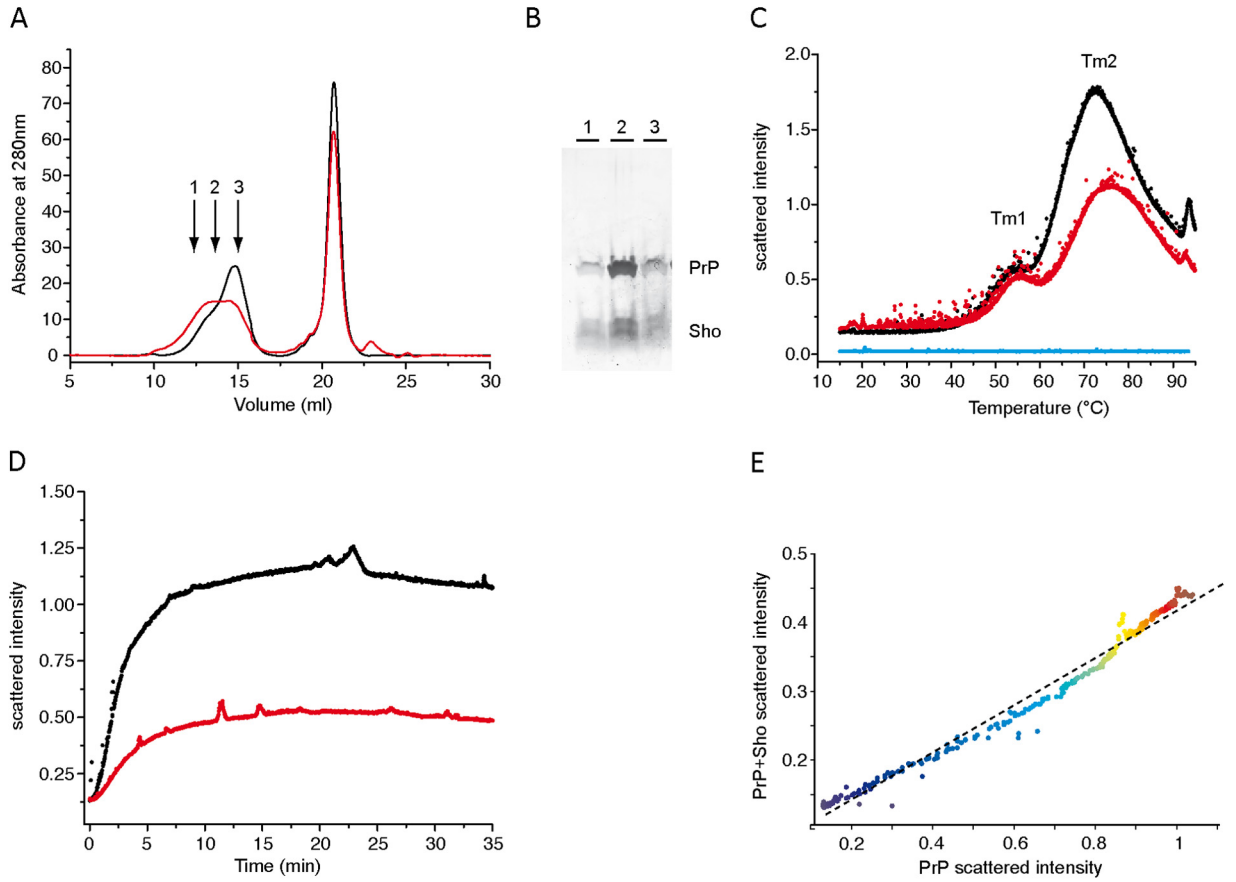

FIG 2 Sho affects the PrP-folding pathway. (A) Results of size-exclusion chromatography analysis of heat-induced oligomerization of 50 μM full-length PrP in the absence of Sho (black line) or in the presence of 10 μM Sho (red line). Arrows indicate fractions 1 to 3 collected to analyze the presence of Sho by SDS-PAGE and Coomassie blue staining (B, lanes 1 to 3, respectively). (A and D) Light-scattering intensity as a function of temperature (C) or as a function of time (D). Black lines, full-length PrP (50 μM); red lines, 50 μM PrP mixed with 10 μM Sho. (E) Correlogram representing the light-scattering intensity of the PrP-Sho mixture as a function of the light-scattering intensity of PrP. The color scale represents time.

2 μM Sho (Fig. 3B, black dots), and the effect of Sho on the infectivity titer was amplified after infection with the 10^{-4} dilution (Fig. 3B, red dots). Indeed, cells treated with 0.6 μM Sho presented a 7-fold increase in the level of PrP^{Sc}. All of the data were statistically significant with regard to the standard deviation. These observations suggest the existence of a range of Sho concentrations at which the conversion process can be either amplified or redirected in a way that enhances the formation of PrP assemblies, which then evolve to form PrP^{Sc}.

DISCUSSION

The contribution of cofactors to the replication process has been suspected since the prion theory was first proposed. Recent observations suggest that the *in vitro* generation of synthetic prions could require the presence of a chaotropic agent, a specific zwitterionic lipid (phosphatidylethanolamine), or RNA fragments (24, 25). Although there are many PrP interactome components (26), little is known about the polypeptide cofactors that can directly bind to PrP and act as ATP-independent holdases (27–29), thereby enhancing prion replication. The broad panel of PrP interactors implies that PrP should be a component of large multimolecular complexes. Sho, a member of the prion protein family, has an internal hydrophobic domain that is homologous to the PrP segment from residues 106 to 126, which has been reported to be involved in interactions with Sho (11). The results presented here characterize, for the first time, the consequence of the PrP-Sho interaction on the PrP-folding landscape and prion conversion process.

Sho's dual binding pathway. Using cross-linking and MST experiments, we show that full-length PrP and Sho are able to form a 1:1 heterodimer, and the biochemical characterization of this interaction using different PrP forms reveals a dual behavior for interactions between Sho and PrP. Sho interacts both with full-length PrP and with the N-terminal domain of PrP, with the K_d being in the micromolar range and the Hill number being 1, suggesting a 1:1 heterocomplex in both cases. However, Sho also cooperatively interacts with the C-terminal domain of PrP (Hill number, >1), which implies that a structural rearrangement of the C-terminal domain of PrP occurs and is then propagated to other PrP C-terminal domain molecules. In other words, oligomerization occurs during the formation of the Sho-PrP complex. Because this cooperativity is not observed with the full-length protein, we concluded that the N terminus of PrP inhibits this cooperativity by affecting the folding dynamics and the PrP oligomerization process. This conclusion was further confirmed by our DSC experiments, which showed that the PrP N-terminal

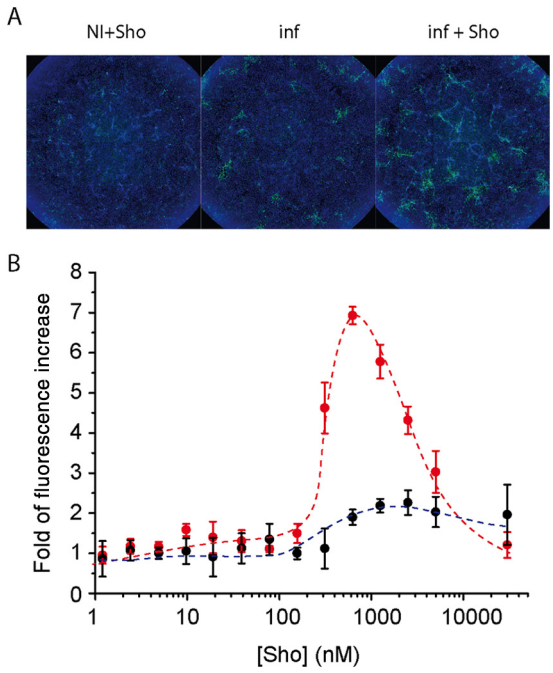

FIG 3 Effect of Sho on PrP conversion in infected cell culture. (A) Representative results of CPT experiments. NI + Sho, noninfected (NI) RK13 cells incubated with 600 nM Sho; inf, cells infected with a 10^{-4} dilution of 127S-infected brain (inf); inf + Sho, RK13 cells incubated with 600 nM Sho and then infected with a 10^{-4} dilution of 127S-infected brain. (B) PrP^{Sc} quantification as a function of the Sho concentration when RK13 cells were infected with a 10^{-3} (black) or 10^{-4} (red) dilution of 127S-infected brain. The results are expressed as the means ± SDs from triplicate experiments and correspond to the ratio of the fluorescence of cells treated with Sho to the fluorescence of nontreated cells.

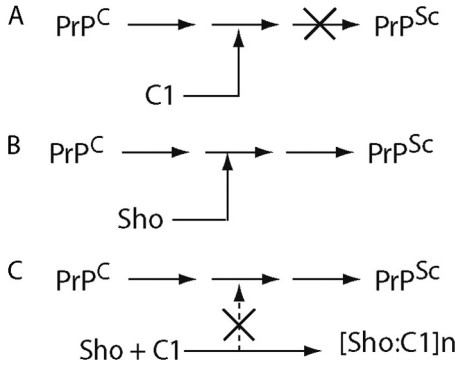

FIG 4 Proposed modes of Sho action on the conversion of PrP^{C} to PrP^{Sc}. (A) PrP truncated form C1 has been reported to act as dominant-negative inhibitor of PrP conversion. (B) By directly interacting with full-length PrP, Sho modifies the PrP-folding pathway and thereby enhances the conversion rate. (C) An allosteric interaction between Sho and PrP truncated form C1 traps C1 in a multimeric complex, switching off the dominant-negative inhibition of C1 and thus enhancing the conversion process.

domain affects the folding dynamics of the C-terminal domain of PrP.

Sho interferes with the PrP-folding pathway and prion replication process. We have previously shown that O1 and O3 are PrP oligomers that are independently generated through two different parallel pathways (22). Here, we highlight that Sho does not affect the O3 oligomerization pathway but drastically affects the O1 oligomerization pathway by decreasing O1 formation. This phenomenon suggests a modification of the PrP-folding landscape by Sho, which may be considered to have an ATP-independent holdase activity. Moreover, as shown in Fig. 2, Sho forms a complex with oligomer O1, leading to the stabilization of its quaternary structure, which suggests that the presence of Sho leads to the formation of more stable O1-Sho assemblies, despite the fact that Sho decreases the rate of O1 formation by affecting the PrP-folding landscape. This dual effect of Sho can be explained by the stabilization of the monomeric state of PrP as well as the oligomeric state of O1. Indeed, the consequence of the stabilization of the monomeric state is a reduction in the oligomerization kinetic when the stabilization of O1 by Sho in the O1-Sho heteroassembly increases the T_m, as shown in Fig. 2C.

CPT showed that Sho is able to enhance the PrP conversion rate. This enhancement was more pronounced at the 10^{-4} than the 10^{-3} inoculum dilution, most likely because infectivity is more efficient and faster at high inoculum concentrations; therefore, we could not show that Sho enhances the conversion process. The last hypothesis could also explain the absence of an effect on the incubation time observed in $Sho^{-/-}$ transgenic mice (30).

Sho may stabilize a PrP^{C} conformer that is more prone to conversion, and Sho-enhanced PrP conversion may also result from its dual binding to PrP. Indeed, the C-terminal C1 fragment has been reported to act as a dominant-negative inhibitor of PrP^{Sc} formation (31). This fragment is derived from physiological PrP proteolytic processing, also called α cleavage, which generates fragments named N1 and C1, which correspond to the N-terminal and C-terminal domains, respectively, of PrP (32, 33). PrP-expressing RK13 cells, including N2a and other PrP-overexpressing cells, that were used in our CPT experiments produce this C1 fragment (31, 34). The cooperative binding of Sho to the C1 fragment traps the fragment and thus interferes with its dominant-negative inhibitor property, which could enhance the replication process. The dual binding behavior of Sho may thus confer regulatory properties on the prion conversion process.

General conclusion. As glycosylphosphatidylinositol-anchored proteins, PrP^{C} and Shadoo may share the same subcellular localization. Both proteins are located on the outside surface of the cell membrane, and they interact with an affinity in the micromolar range, which strongly suggests an association of their respective activities under physiological conditions.

The results described in this work strongly suggest a contribution of Sho to the prion conversion process. This contribution could occur through either (i) a direct interaction with full-length PrP that leads to a more stable heterocomplex exhibiting a quaternary structure different from the one formed in the absence of Sho (Fig. 4A) or (ii) a second pathway by which Sho can target the C1 fragment. The latter has been reported to act as a dominant-negative inhibitor (Fig. 4B). The allosteric interaction of Sho with the PrP C-terminal fragment switches off the dominant-negative inhibitor effect of C1 and thus enhances the prion conversion rate (Fig. 4C).

ACKNOWLEDGMENTS

This work was supported by INRA, the Délégation Générale pour l'Armement (DGA), and the Laboratoire du Fractionnement des Produits Biologiques (LFB). D.C. was supported by a scholarship from the French Ministry of Foreign Affairs and International Development.

REFERENCES

1. **Büeler H, Aguzzi A, Sailer A, Greiner RA, Autenried P, Aguet M, Weissmann C.** 1993. Mice devoid of PrP are resistant to scrapie. Cell **73:**1339–1347. http://dx.doi.org/10.1016/0092-8674(93)90360-3.
2. **Watts JC, Drisaldi B, Ng V, Yang J, Strome B, Horne P, Sy M, Yoong L, Young R, Mastrangelo P, Bergeron C, Fraser PE, Carlson GA, Mount HTJ, Schmitt-Ulms G, Westaway D.** 2007. The CNS glycoprotein Shadoo has PrP(C)-like protective properties and displays reduced levels in prion infections. EMBO J **26:**4038–4050. http://dx.doi.org/10.1038/sj.emboj.7601830.
3. **Young R, Le Guillou S, Tilly G, Passet B, Vilotte M, Castille J, Beringue V, Le Provost F, Laude H, Vilotte J-L.** 2011. Generation of Sprn-regulated reporter mice reveals gonadic spatial expression of the prion-like protein Shadoo in mice. Biochem Biophys Res Commun **412:**752–756. http://dx.doi.org/10.1016/j.bbrc.2011.08.049.
4. **Passet B, Young R, Makhzami S, Vilotte M, Jaffrezic F, Halliez S, Bouet S, Marthey S, Khalifé M, Kanellopoulos-Langevin C, Béringue V, Le Provost F, Laude H, Vilotte J-L.** 2012. Prion protein and Shadoo are involved in overlapping embryonic pathways and trophoblastic development. PLoS One **7:**e41959. http://dx.doi.org/10.1371/journal.pone.0041959.
5. **Moore RC, Lee IY, Silverman GL, Harrison PM, Strome R, Heinrich C, Karunaratne A, Pasternak SH, Chishti MA, Liang Y, Mastrangelo P, Wang K, Smit AF, Katamine S, Carlson GA, Cohen FE, Prusiner SB, Melton DW, Tremblay P, Hood LE, Westaway D.** 1999. Ataxia in prion protein (PrP)-deficient mice is associated with upregulation of the novel PrP-like protein doppel. J Mol Biol **292:**797–817. http://dx.doi.org/10.1006/jmbi.1999.3108.
6. **Premzl M, Sangiorgio L, Strumbo B, Marshall Graves JA, Simonic T, Gready JE.** 2003. Shadoo, a new protein highly conserved from fish to mammals and with similarity to prion protein. Gene **314:**89–102. http://dx.doi.org/10.1016/S0378-1119(03)00707-8.
7. **Young R, Passet B, Vilotte M, Cribiu EP, Béringue V, Le Provost F, Laude H, Vilotte J-L.** 2009. The prion or the related Shadoo protein is required for early mouse embryogenesis. FEBS Lett **583:**3296–3300. http://dx.doi.org/10.1016/j.febslet.2009.09.027.
8. **Daude N, Wohlgemuth S, Brown R, Pitstick R, Gapeshina H, Yang J, Carlson GA, Westaway D.** 2012. Knockout of the prion protein (PrP)-like Sprn gene does not produce embryonic lethality in combination with PrPC-deficiency. Proc Natl Acad Sci U S A **109:**9035–9040. http://dx.doi.org/10.1073/pnas.1202130109.
9. **Daude N, Ng V, Watts JC, Genovesi S, Glaves JP, Wohlgemuth S, Schmitt-Ulms G, Young H, McLaurin J, Fraser PE, Westaway D.** 2010. Wild-type Shadoo proteins convert to amyloid-like forms under native conditions. J Neurochem **113:**92–104. http://dx.doi.org/10.1111/j.1471-4159.2010.06575.x.
10. **Westaway D, Genovesi S, Daude N, Brown R, Lau A, Lee I, Mays CE, Coomaraswamy J, Canine B, Pitstick R, Herbst A, Yang J, Ko KWS, Schmitt-Ulms G, Dearmond SJ, McKenzie D, Hood L, Carlson GA.** 2011. Down-regulation of Shadoo in prion infections traces a pre-clinical event inversely related to PrP(Sc) accumulation. PLoS Pathog **7:**e1002391. http://dx.doi.org/10.1371/journal.ppat.1002391.
11. **Jiayu W, Zhu H, Ming X, Xiong W, Songbo W, Bocui S, Wensen L, Jiping L, Keying M, Zhongyi L, Hongwei G.** 2010. Mapping the interaction site of prion protein and Sho. Mol Biol Rep **37:**2295–2300. http://dx.doi.org/10.1007/s11033-009-9722-0.
12. **Rezaei H, Marc D, Choiset Y, Takahashi M, Hui Bon Hoa G, Haertlé T, Grosclaude J, Debey P.** 2000. High yield purification and physico-chemical properties of full-length recombinant allelic variants of sheep prion protein linked to scrapie susceptibility. Eur J Biochem **267:**2833–2839. http://dx.doi.org/10.1046/j.1432-1033.2000.01347.x.
13. **Baaske P, Wienken CJ, Reineck P, Duhr S, Braun D.** 2010. Optical thermophoresis for quantifying the buffer dependence of aptamer binding. Angew Chem Int Ed Engl **49:**2238–2241. http://dx.doi.org/10.1002/anie.200903998.
14. **Zillner K, Jerabek-Willemsen M, Duhr S, Braun D, Längst G, Baaske P.** 2012. Microscale thermophoresis as a sensitive method to quantify protein: nucleic acid interactions in solution. Methods Mol Biol **815:**241–252. http://dx.doi.org/10.1007/978-1-61779-424-7_18.
15. **Jerabek-Willemsen M, Wienken CJ, Braun D, Baaske P, Duhr S.** 2011. Molecular interaction studies using microscale thermophoresis. Assay Drug Dev Technol **9:**342–353. http://dx.doi.org/10.1089/adt.2011.0380.
16. **Duhr S, Braun D.** 2006. Why molecules move along a temperature gradient. Proc Natl Acad Sci U S A **103:**19678–19682. http://dx.doi.org/10.1073/pnas.0603873103.
17. **Rezaei H, Eghiaian F, Perez J, Doublet B, Choiset Y, Haertle T, Grosclaude J.** 2005. Sequential generation of two structurally distinct ovine prion protein soluble oligomers displaying different biochemical reactivities. J Mol Biol **347:**665–679. http://dx.doi.org/10.1016/j.jmb.2005.01.043.
18. **Vilette D, Andreoletti O, Archer F, Madelaine MF, Vilotte JL, Lehmann S, Laude H.** 2001. Ex vivo propagation of infectious sheep scrapie agent in heterologous epithelial cells expressing ovine prion protein. Proc Natl Acad Sci U S A **98:**4055–4059. http://dx.doi.org/10.1073/pnas.061337998.
19. **Tixador P, Herzog L, Reine F, Jaumain E, Chapuis J, Le Dur A, Laude H, Béringue V.** 2010. The physical relationship between infectivity and prion protein aggregates is strain-dependent. PLoS Pathog **6:**e1000859. http://dx.doi.org/10.1371/journal.ppat.1000859.
20. **Paquet S, Langevin C, Chapuis J, Jackson GS, Laude H, Vilette D.** 2007. Efficient dissemination of prions through preferential transmission to nearby cells. J Gen Virol **88:**706–713. http://dx.doi.org/10.1099/vir.0.82336-0.
21. **Rezaei H, Choiset Y, Eghiaian F, Treguer E, Mentre P, Debey P, Grosclaude J, Haertle T.** 2002. Amyloidogenic unfolding intermediates differentiate sheep prion protein variants. J Mol Biol **322:**799–814. http://dx.doi.org/10.1016/S0022-2836(02)00856-2.
22. **Eghiaian F, Daubenfeld T, Quenet Y, van Audenhaege M, Bouin A-P, van der Rest G, Grosclaude J, Rezaei H.** 2007. Diversity in prion protein oligomerization pathways results from domain expansion as revealed by hydrogen/deuterium exchange and disulfide linkage. Proc Natl Acad Sci U S A **104:**7414–7419. http://dx.doi.org/10.1073/pnas.0607745104.
23. **Chakroun N, Prigent S, Dreiss CA, Noinville S, Chapuis C, Fraternali F, Rezaei H.** 2010. The oligomerization properties of prion protein are restricted to the H2H3 domain. FASEB J **24:**3222–3231. http://dx.doi.org/10.1096/fj.09-153924.
24. **Deleault NR, Walsh DJ, Piro JR, Wang F, Wang X, Ma J, Rees JR, Supattapone S.** 2012. Cofactor molecules maintain infectious conformation and restrict strain properties in purified prions. Proc Natl Acad Sci U S A **109:**E1938–E1946. http://dx.doi.org/10.1073/pnas.1206999109.
25. **Deleault NR, Harris BT, Rees JR, Supattapone S.** 2007. Formation of native prions from minimal components in vitro. Proc Natl Acad Sci U S A **104:**9741–9746. http://dx.doi.org/10.1073/pnas.0702662104.
26. **Nieznanski K.** 2010. Interactions of prion protein with intracellular proteins: so many partners and no consequences? Cell Mol Neurobiol **30:**653–666. http://dx.doi.org/10.1007/s10571-009-9491-2.
27. **Rikhvanov EG, Romanova NV, Chernoff YO.** 2007. Chaperone effects on prion and nonprion aggregates, p 83–89. *In* Chernoff YO (ed), Protein-based inheritance. Landes Bioscience, Austin, TX.
28. **Hartl FU, Bracher A, Hayer-Hartl M.** 2011. Molecular chaperones in protein folding and proteostasis. Nature **475:**324–332. http://dx.doi.org/10.1038/nature10317.
29. **Fu X.** 2014. Chaperone function and mechanism of small heat-shock proteins. Acta Biochim Biophys Sin (Shanghai) **46:**347–356. http://dx.doi.org/10.1093/abbs/gmt152.
30. **Li S, Ju C, Han C, Li Z, Liu W, Ye X, Xu J, Xulong L, Wang X, Chen Z, Meng K, Wan J.** 2014. Unchanged survival rates of Shadoo knockout mice after infection with mouse-adapted scrapie. Prion **8:**339–343. http://dx.doi.org/10.4161/19336896.2014.971574.
31. **Westergard L, Turnbaugh JA, Harris DA.** 2011. A naturally occurring C-terminal fragment of the prion protein (PrP) delays disease and acts as a dominant-negative inhibitor of PrPSc formation. J Biol Chem **286:**44234–44242. http://dx.doi.org/10.1074/jbc.M111.286195.
32. **Chen SG, Teplow DB, Parchi P, Teller JK, Gambetti P, Autilio-Gambetti L.** 1995. Truncated forms of the human prion protein in normal brain and in prion diseases. J Biol Chem **270:**19173–19180. http://dx.doi.org/10.1074/jbc.270.32.19173.
33. **Jiménez-Huete A, Lievens PM, Vidal R, Piccardo P, Ghetti B, Tagliavini F, Frangione B, Prelli F.** 1998. Endogenous proteolytic cleavage of normal and disease-associated isoforms of the human prion protein in neural and non-neural tissues. Am J Pathol **153:**1561–1572. http://dx.doi.org/10.1016/S0002-9440(10)65744-6.
34. **Beringue V, Vilette D, Mallinson G, Archer F, Kaisar M, Tayebi M, Jackson GS, Clarke AR, Laude H, Collinge J, Hawke S.** 2004. PrPSc binding antibodies are potent inhibitors of prion replication in cell lines. J Biol Chem **279:**39671–39676. http://dx.doi.org/10.1074/jbc.M402270200.